Pergamon

Tetrahedron Vol. 51, No. 25, pp. 6855-6868, 1995

0040-4020/95 $9.50+0.00

0040-4020(95)00333-9

Structure and Dynamics of MMI Linked Nucleotides

Venkatraman Mohan[1*], Richard H. Griffey[1] and Darrell R. Davis[2]

[1]ISIS Pharmaceuticals, 2292 Faraday Avenue, Carlsbad, CA 92008

[2]Department of Medicinal Chemistry, University of Utah, Salt Lake City, UT 84112

Key words: antisense therapeutics; neutral MMI linker; NMR; molecular dynamics; conformational analysis

Abstract: *Results are presented on molecular dynamics (MD) simulations of (T*T) dimers linked by a novel chemical functionality -- the methylene methyl imino (MMI) backbone designed as a neutral replacement for the negatively charged phosphodiester group in wild type nucleic acids. Simultaneous conformational transitions among the MMI backbone atoms during the course of the simulation have been observed, equivalent to inversion-rotation at the nitrogen atoms of the N-O bond. This process yields two families of low-energy conformations which maintain base stacking. The solution structure of the dimer has been studied by one and two-dimensional ^1H NMR spectroscopy, and two slowly exchanging forms are observed at low temperature. Simulated NOESY spectra generated from the MD structures match the experimental NOESY data.*

INTRODUCTION

Considerable progress has been made (1) in exploring the potential of 'antisense' therapeutic applications. The antisense technique (2) involves binding of a single-stranded synthetic oligonucleotide to mRNA, in a sequence specific manner with high affinity. Several properties of wild-type nucleotides must be improved for antisense technology to succeed (3), including stability of the resulting duplex, increased cellular permeation, and decreased rates of degradation by nucleases that cleave the phosphate backbone. A variety of chemical modifications have been prepared to modulate these characteristics, including alterations in the nucleobase (4), conversion of the deoxyribose to a six-membered hexose (5) or morpholino

group (6), and replacement of the phosphate backbone (7). However, only a limited number of conformational studies have been reported for such modifications (7g,h).

The neutral, achiral MMI backbone (**Figure 1**) has been prepared as a potential substitute for the phosphate group. MMI-linked thymidine dimers (T*T) have been synthesized and incorporated into antisense oligomers, and their hybridization properties evaluated against complementary RNAs (7a). Incorporation of the MMI-linked nucleotides results in a more stable heteroduplex with sequence specificity equivalent to wild-type DNA(7i). MMI dinucleotides are refractory to nucleases, and confer significant endo- and exonuclease resistance onto flanking phosphodiesters (8).

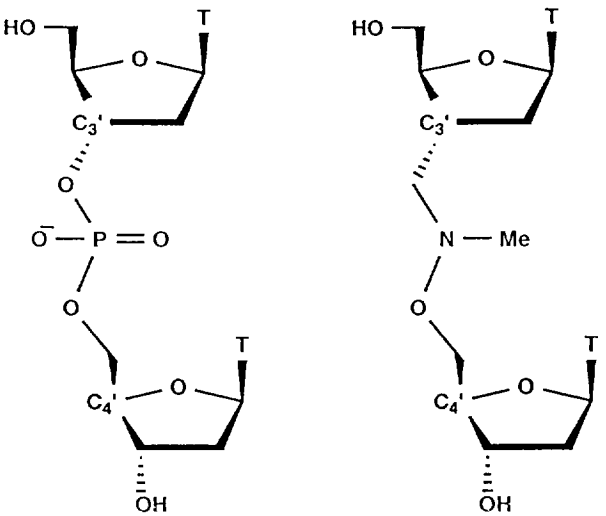

(a) Phosphodiester linker (b) MMI linker

Figure 1. (a) Negatively charged chiral wild-type phosphodiester and (b) neutral achiral MMI functional groups along nucleic acid backbone.

We report herein the results of conformational analysis of MMI-linked nucleotides (T*T) investigated by MD simulation techniques in the presence of explicit solvent. Two families of structures are observed, related by inversion-rotation at the hydroxylamine nitrogen. Two slowly exchanging conformations are detected at low temperature using proton NMR spectroscopy. NOESY spectra calculated from the low energy MD structures match the experimental NOESY data. The observation of two geometries for the MMI backbone suggests that multiple conformations of the antisense strand may form stable duplexes, not limited to canonical A and B forms.

METHODS

General

All computations have been performed on a Silicon Graphics (Mountain View) Indigo^2 workstation. The conformational search, MD simulations, and analyses have been carried out using the InsightII/Discover software package of BIOSYM Technologies (San Diego).

NMR Studies

Proton NMR studies were conducted using a 400 MHz Unity spectrometer (Varian Associates, Palo Alto). A 2.5 mg sample of **1b** (**Figure 1**) was dissolved in 500 μL of deuterium oxide. The sample was diluted with 250 μL of [D-4] methanol for variable temperature studies. The 3-bond proton-proton coupling constants from each furanose ring were measured directly or determined using the Varian spin simulation routine. The PSEUDOROT program of Altona and co-workers was modified to account for the substituents of each sugar (9). The H1'-H2', H2'-H3', and H3'-H4' coupling constants were fit via a non-linear least squares procedure to a two-state exchange model, yielding values for a 'northern' sugar pucker P_n, a 'southern' sugar pucker P_S, and the % of the sugar in the northern conformation.

Two-dimensional (2D) NOESY spectra were acquired and processed in a phase-sensitive manner (10). Typically, a total of 4096x1024 hypercomplex data points were obtained and weighted with a shifted sine bell prior to Fourier transformation. Proton chemical shifts were determined relative to methanol, and expressed relative to TMS. Spectral assignments were established from 2D TOCSY experiments at 40°C and at -30°C (11).

NOESY spectra were calculated from refined structures using the program BKCALC (Hare Research, Bothell). BKCALC simulates the NOESY spectrum by numerical integration of the Bloch equations for a relaxation network defined by the coordinates of a molecular structure. The details of this procedure have been described (12). The cross-relaxation and leackage rate parameters for the simulation were iteratively optimized for a conformer based on the cross-peak build up rates simultaneously with the autopeak decay. The same relaxation parameters were then used to back-calculate the spectrum for other conformers. An interproton cutoff distance of 5 Å and a time increment of 1 msec was used for all the BKCALC simulations.

Conformational Search

A wild type nucleotide in the standard C2'-endo conformation has been modified to an MMI linked nucleotide (T*T) by appropriate atom substitutions. A conformational search of this dimer has been performed using a quenched molecular dynamics (MD) protocol. The permitivity has been modulated by employing a distance-dependent dielectric function [$\varepsilon = 4 \cdot r_{ij}$]. The system was heated initially to 1000 K, to provide enough kinetic energy to sample the entire conformational space. The simulation was carried out for a period of 20 ps, and at this point, the system was quenched to 300 K, subjected to energy minimization, and the

resulting structure stored. This process was repeated for a total of 1 ns, generating 51 frames for further scrutiny. The results of the conformational search are shown in **Figure 2.**

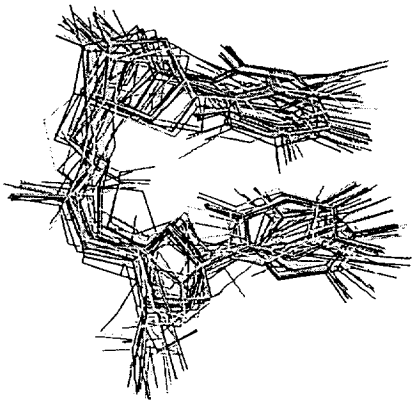

Figure 2. MMI linked (T^*T) dimer. Superimposed structures collected during quenched MD simulation. Hydrogens are omitted.

Frames were partitioned into two classes, with the N-Me group pointing "**out**" (conformer I) and N-Me group pointing "**in**" (conformer **II**) based on energy. From these families of structures, two degenerate conformers with the lowest energy were chosen as initial structures for MD simulations with explicit solvent. The stereo views are presented with the N-Me group pointing "**out**" **[Figure 3a]** and N-Me group pointing "**in**" **[Figure 3b].**

Molecular Dynamics

MD simulation results are highly dependent on the initial structure, and repeating the simulations with different starting structures aids in understanding the dynamic behavior of the system under investigation. Since no energy difference was observed between the two lowest energy states identified in the conformational search described above, we have performed two independent MD simulations with each as initial configurations.

One of the lowest energy conformers of the MMI linked nucleotide (conformer **I**) was placed in a cubical box of side length 20.0 Å filled with pre-equilibrated water molecules. Those solvent molecules in steric clash with the solute were deleted. The 234 water molecules left in the central simulation box yields a density of approximately 1 g cm^{-3}. MD simulations have been carried out under periodic boundary conditions with a 1 fs time step, at constant volume and a constant temperature of 300 K. A 10 Å cutoff has been used in computing the intermolecular interactions. All specific 1-4 nonbonded interaction energy terms have been scaled by a factor of 0.5. A three-point flexible water model has been employed in our calculations. A dielectric constant of 1.0 was used throughout the calculations. Electrostatic interactions were computed using partial atomic charges (13) and Coulomb's law. Our present MD simulations were carried out with the AMBER all-atom force field (14), including appropriate modifications to incorporate the N-O parameters (15). An identical

protocol was followed in the second simulation with conformer **II** as the starting structure of the MMI linked nucleotide.

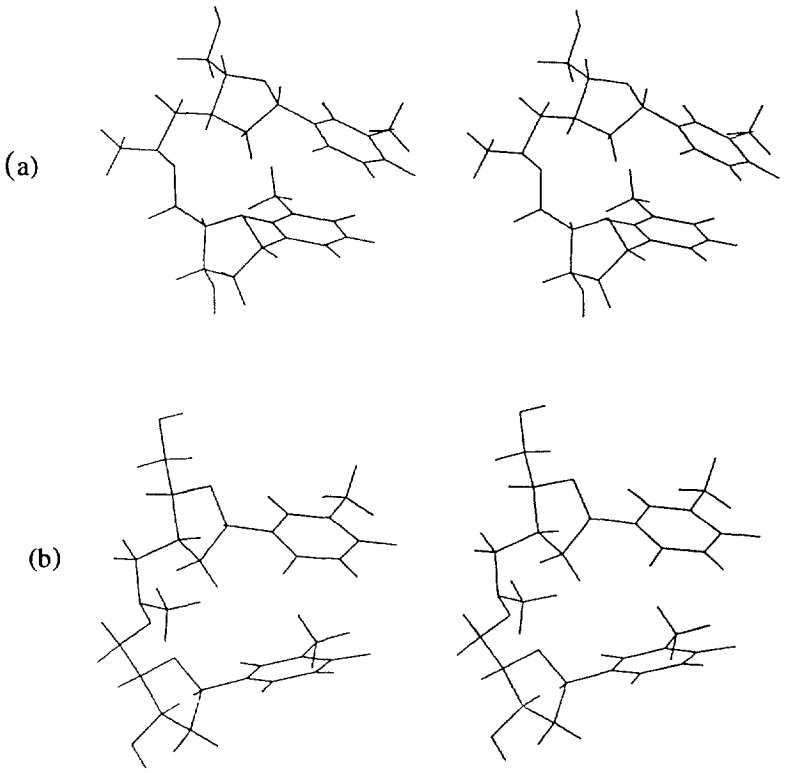

Figure 3. Stereo view of initial structures used in the MD simulations. (a) N-Me group pointing "out" (b) N-Me group pointing "in". These are also the low energy degenerate conformers identified in the conformational search scheme.

A 190 ps MD simulation has been performed in three stages. The MD simulation was initiated by 1000 steps of steepest descent energy minimization of the solvent. The nucleotide was held fixed for the initial 15 ps, allowing the solvent to move freely. Another 75 ps of MD simulation was carried out holding the nucleobases fixed and letting the backbone of the nucleotide relax. Finally, 100 ps of data collection followed, setting the whole system in free motion. A similar MD protocol has been employed in a number of recent studies (16,17) to ensure that no metastable solvent structures are produced (18) which are slow to dissipate. The system remained energetically stable after the equilibration phase. The analyses have been performed on the final 100 ps of the MD simulation.

RESULTS AND DISCUSSIONS

NMR Studies

The conformational properties of the furanose rings in the MMI dimer have been estimated using NMR. The 3-bond proton-proton coupling constants for both sugars at 20°C are listed in Table I, along with the calculated values for P_N, P_S, and %N. The 5'-dT residue adopts an 'N' pucker, while the 3'-dT is best fit to an 'S' geometry. The pucker amplitude of the 5'-sugar was varied from 34° to 40° to explore potential alterations induced by the 3'-methylene substituent. The values for P_N, P_S, and %N varied by less than 10° and 3%, respectively (data not shown). A 37° pucker amplitude generated the best fit to the experimental data for both sugars.

Table I. Proton NMR Coupling Constants for MMI T*T Dimer and Calculated Pseudorotation Parameters.

Sugar Residue	JH1'H2'	JH1'H2"	JH2'H3'	JH3'H4'	P_N	P_S	%N
3'-dT	6.4	6.8	4.8	3.5	-13	157	26.5
5'-dT	3.4	6.4	5.3	5.6[a]	-5	140	66.5

a. Best fit from spin simulation.

^{1}H NMR studies of the MMI dimer performed as a function of temperature suggest two conformations of the backbone exist in solution. At 20°C, the resonances from the H6 protons of the pyrimidines, at 7.98 (5'-sugar) and 7.73 ppm (3'-sugar), are relatively sharp signals, as shown in **Figure 4a**. As the temperature is reduced to 5° and then to -20°C(**Figure 4b** and **4c**), the resonance from the H6 proton of the 5'-dT broadens rapidly, and splits into two peaks at -30°C (**Figure 4d**). The signal from the H6 proton of the 3'-dT broadens and resolves into two peaks more slowly. In addition, the chemical shift for this proton moves upfield, as the degree of stacking among the bases increases. At -30°C, the signals from both H6 protons resolve into two peaks, centered at 7.95 and 7.61 ppm, respectively. The ratio of the two conformers is ~60:40, consistent with a small energetic barrier for interconversion. Further reduction to -50°C produces no change in the appearance of the spectrum. Attempts to measure proton coupling constants between -30 and -50°C were unsuccessful given the linewidth of ~2 Hz, but all resonances could be assigned from 2D TOCSY spectra obtained at -30°C and 20°C with a 50 msec spin lock period. The chemical shifts observed for all protons at -30°C are listed in Table II.

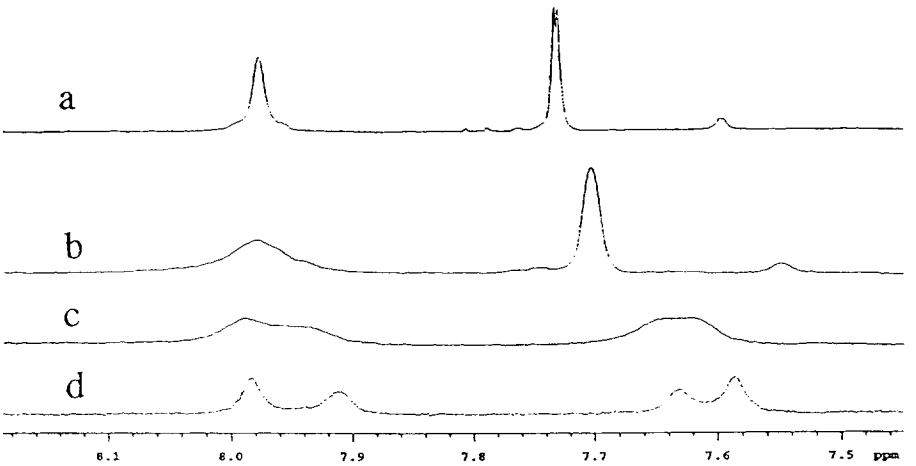

Figure 4. Proton NMR spectra of the MMI T*T dimer **1b** obtained as a function of sample temperature. Spectra obtained at a) 20°C; b) 5°C; c) -20°C, d) -30°C.

Table II. List of proton chemical shift assignments for Conformers **I** and **II** at -30°C.

Proton	Chemical Shift (ppm) Conformer I	Conformer II
3' dT		
H6	7.60	7.66
H1'	6.09	6.25
H2'	2.27	2.36
H2"	2.47	2.36
H3'	4.38	4.45
H4'	4.23	4.07
H5'	3.95	3.93
H5"	3.72	3.93
Me	1.92	1.90
5'dT		
H6	8.02	7.95
H1'	6.05	6.09
H2'	2.35	2.39
H2"	2.50	2.40
H3'	2.71	2.57
H4'	3.89	3.92
H5'	3.90	3.82
H5"	3.73	3.82
Me	1.79	1.88
H3"	2.95	2.93
H3"'	2.84	2.85
NMe	2.78	2.70

A low-temperature NOESY experiment has been performed to determine structural differences between the two conformations. A section from the NOESY spectrum obtained at -30°C is presented in **Figure 5A.** In the major form, strong NOE cross-peak intensity is observed from the H6 protons to their respective methyl, H1', and H3' protons, as expected

for nucleoside residues with 'N' sugar puckers. Both H6 protons of the major form generate cross-peaks to the H3' proton of the 5' sugar at 2.71 ppm. Additional signals are observed from the respective H6 protons to their own H2' proton, and from H6 of the 3'-residue to the H2" proton of the 5'-residue. For the major conformation, a 3-fold enhancement in NOE cross-peak intensity is observed from the H6 proton of the 3'-nucleoside at 7.6 ppm to the H5" proton at 3.72 ppm.

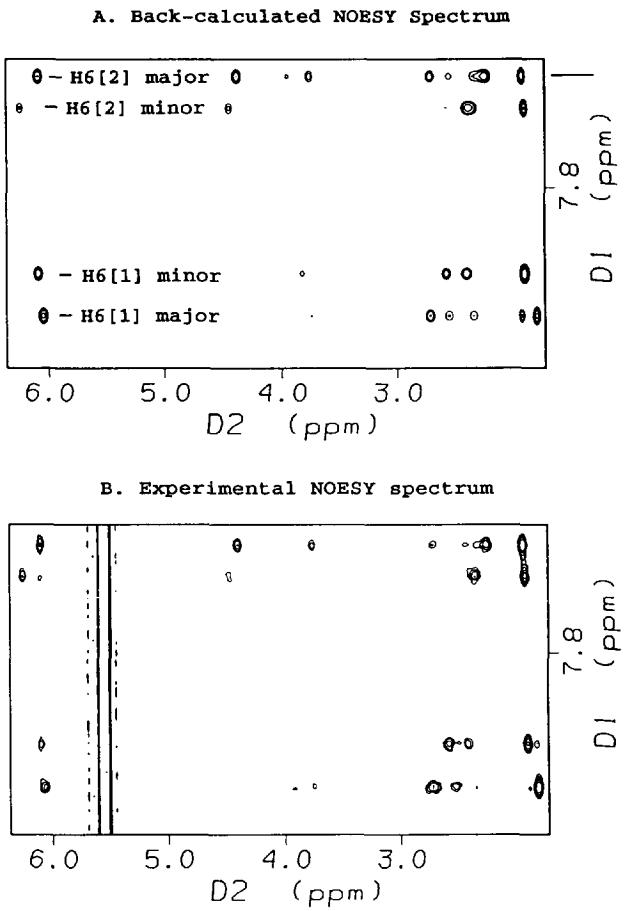

Figure 5. (A) Section of the BKCALC NOESY spectrum for 1b calculated for a mixture of the major and minor conformers using a 150 msec mixing time. (B) Section of the experimental 2D NOESY spectrum for 1b obtained at -31°C. A total of 4096X1024 hypercomplex points were acquired using a 4 KHz sweep width and multiplied by a sine bell shifted by $\pi/2$ radinans prior to Fourier transformation in each dimension. A mixing time of 150 msec was employed with a repetition time of 4.0 sec.

Other NOESY cross peak intensities are within 25% for both conformers, including the cross-peak intensity from each H6 proton to the respective H1', H2', and H3' protons. These results suggest that a major structural difference between the two conformations observed by NMR at -30°C involves the rotation of the γ dihedral from a g^+ to a t geometry, bringing the H5" proton into proximity of the H6 proton. In the minor form, inversion-rotation at nitrogen shifts the H3"' proton away from the 3'-residue, with a loss in NOE intensity between the 3'-H6 proton (7.66 ppm) and the 5'-H3"' proton (2.85 ppm).

The NOESY spectra predicted for each of the two conformers obtained from the MD search were determined independently using BKCALC. The two data matrices were added to create the composite spectrum from the conformer I and conformer II forms shown in **Figure 5B**. Relaxation parameters for the back-calculation were identical for the two conformers. Analysis of the calculated spectrum shows that the determined structures are consistent with the experimetntal data and also reflect the general differences between the two conformational forms. In the major form, strong NOE intensity is predicted from the H3' proton of the 5' sugar and both H6 protons. The back-calculated spectrum accurately predicts the observed NOE patterns from the H2',2" protons of both sugars to the aromatic protons. The different NOE patterns observed from the 3'-H6 proton of the major and minor forms to the H5" proton of the 3'-sugar are reproduced. There are minor differences between the calculated and exerimental data; the principle reason for this is the difficulty in accurately modeling the relaxation behavior for a dinucleotide system. For large DNA duplexes, a single correlation time accurately describes most of the system and the "ends" are often omitted (19). In this dinucleotide sytstem, it was somewhat more difficult to allow for local molecular motion, but the simulation clearly validates the major structural features. Back-calcualted spectra generated from variants of the major or minor form alone could not be fit to the experimental data.

Backbone Conformational Transitions

A set of new torsion angles along the MMI backbone is defined and shown in **Figure 6**. The time-averaged values of the individual backbone torsion angles are listed in Table III. The only relevant conformational change in the backbone observed during the MD simulations involves the angles α and γ. **Figure 7** shows the time history of α and γ during the final 100 ps of the present simulation. At 150 ps, a conformational transition in α from (g^-) to (t) occurs in form A. Simultaneously, a transition in γ from (g^+) to (t) has been observed. However, around 178 ps, the reverse transitions in α [from (t) to (g^-)] and γ [from (t) to (g^+)] become apparent. The average values and the standard deviations listed in Table III are manifestations of these transitions. Such correlated transitions among the backbone atoms in nucleic acid simulations have been observed (20). Smaller standard deviations for different torsion angles along the MMI backbone reflect the conserved motion at the β and δ dihedrals relative to the larger motions at the α and γ positions.

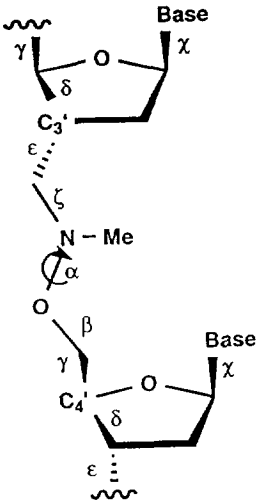

Figure 6. Definition of various torsional angles along MMI backbone atoms.

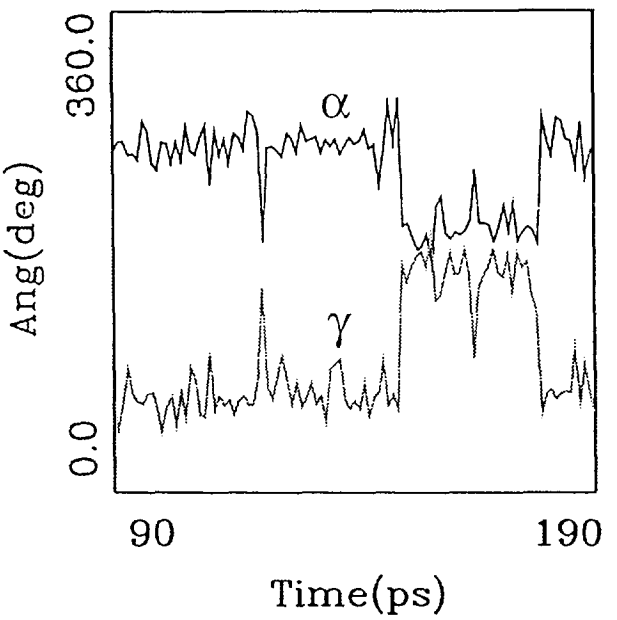

Figure 7. Time history of the torsional angles α and γ during the course of MD simulation. Simultaneous conformational transitions in both α and γ are observed at time =150 ps and 178 ps.

Table III. Backbone torsion angles* (in degrees) averaged over the final 100 ps of MD simulation.The standard deviations are given in parentheses.

System	α	β	γ	δ	ε	ζ
Wild type	−81.3 (13.2)	74.5 (21.0)	159.9 (34.3)	135.6 (18.3)	−80.7 (10.5)	241 (69.0)
N-Me out	-118.3 (31.8)	-179.4 (8.0)	99.3 (43.5)	82.5 (12.2)	-175.0 (10.3)	-63.3 (11.0)
N-Me in	-106.0 (22.8)	-175.8 (8.6)	81.8 (31.3)	87.8 (14.6)	-168.7 (13.7)	-60.2 (13.8)

* See Figure 6 for definitions.

Sugar Puckering

An important structural feature of nucleic acid is the puckering of the five-membered furanose rings. In B-form helical structures, the furanose rings assume a C_2'-endo puckering (S-type), while in A-form helices the C_3'-endo pucker (N-type) is favored. The torsional angle δ correlates strongly with the sugar puckering conformation. In general, the value of δ

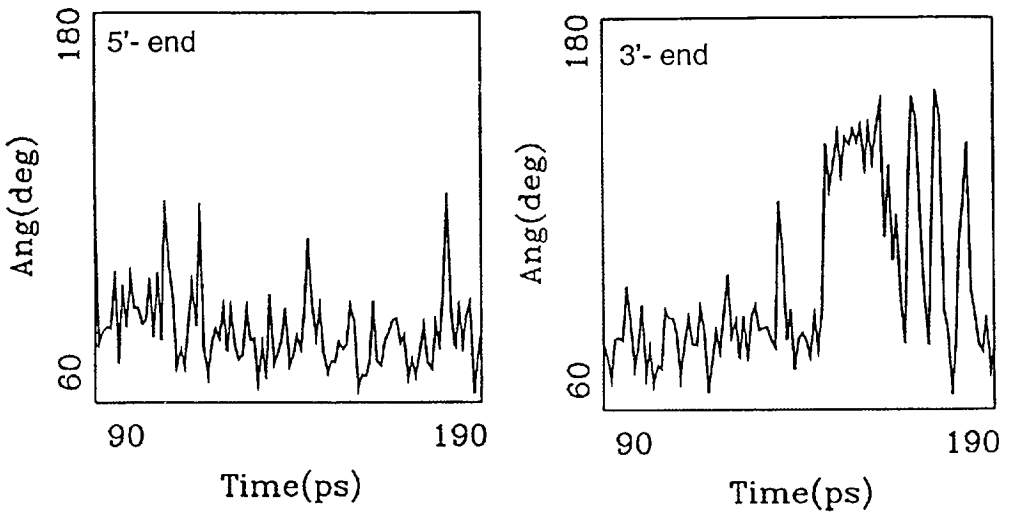

Figure 8. Variation of the torsional angle d of 5'-end and 3'-end furanose rings as a function of time.

for a $C3'$-endo conformation lies between 70° and 85°, and for $C2'$-endo lies between 140° and 160° (21). Time histories of the δ torsional angles of the 5'-end and 3'-end of the MMI linked nucleotide are shown in **Figure 8**. The 5'-end of the sugar is predominantly in an RNA-like conformation whereas the 3'-end deoxyribose unit transits between N and S puckered states. The NMR experimental results indicate that the 5'-end furanose is 66.5% N puckered whereas the 3'-end deoxyribose is only 26.5% N. Despite the fact that the initial structure MMI linked nucleotide has been model-built to be in B-form DNA, the 5'-end preferentially adopts an N-type sugar pucker, in agreement with the NMR results.

CONCLUSIONS

Conformational searches performed using quenched MD and 2D low-temperature NMR studies suggest that the backbone in an MMI-linked T*T dinucleotide can adopt two low-energy forms, which differ through inversion-rotation at nitrogen. Both conformers can assume geometries with the reduced steric bulk of the MMI backbone relative to phosphate. The proton NMR spectrum contains resolved signals from two distinct species, which are in fast exchange above 20°C and are in slow exchange at low-temperature. The low-temperature NOE pattern observed from the aromatic and sugar protons are consistant with structures having the T bases stacked, but with altered backbone dihedrals. The experimental NOE spectrum is reproduced by mixing data from two low energy conformers observed in the quenched MD analysis.

MD simulations have been performed with these conformers as initial structures in the presence of explicit solvent to provide insight into the dynamical nature of the MMI linker and its influence on the puckering modes of the sugar moieties. The correlated transitions observed for the α and γ dihedrals in the MMI backbone (present along the backbone) suggest that MMI-linked nucleotides may have increased flexibility. This motion is offset by the low motion about the β and δ dihedrals. The backbone dihedral angles of the major conformer of the MMI unit do not match those of a conventional phosphodiester. This difference and altered flexibility may play a key role in affording the observed nuclease stability of the MMI dimer incorporated duplexes (8). The altered backbone dihedrals would not affect the affinity for complement, since the base stacking and geometry is maintained in both forms. The 5'-end of the sugar exists predominantly in RNA-like conformation whereas in the 3'-end deoxyribose unit, frequent transitions between N and S puckered states have been observed during the course of the simulation. The results are in close agreement with values for the sugar pucker determined from fitting of NMR coupling constants. It may be possible to preferentially lock the conformation of the 3'-end furanose ring through suitable modification, which would further enhance the binding of MMI oligomers to target RNA strands.

Acknowledgments

We wish to thank Dr. Yogesh Sanghvi for preparation of a sample of the MMI T*T dimer for NMR analysis. We also wish to thank Dr.Tom Thatcher for helpful discussions.

References

1. Crooke, S.T.; *Curr.Opin.Invest.Drugs*, **1993**, *2*, 1045-1048.
2. Uhlmann, E.; Peyman, A.; *Chem.Rev.* **1990**,*90*, 543-584.
3. "Antisense Research and Applications", Ed. Crooke,S.T. and Lebleu, B. CRC Press, Florida, **1993**.
4. Varma, R.S.; *SYNLETT*, **1993**, 621-637.
5. Pitsch, S.; Wendeborn, S.; Jaun B.; Eschenmoser, A.; *Helv. Chimi. Acta* ,**1993**,*76*, 2161-2183.
6. Weller, D.D.; Daly, D.T.; Olson, W.K.; Summerton, J.E.; *J.Org.Chem.*,**1991**,*56*, 6000-6007.
7. (a) Vasseur, J.-J.; Debart, F.; Sanghvi,Y.S.; Cook, P.D.; *J.Am.Chem.Soc.*, **1992**,*114*, 4006-4007. (b) Debart, F.; Vasseur, J.-J.;Sanghvi, Y.S.; Cook, P.D.; *Bioorg.Med.Chem.Lett.*, **1992**,*2*, 1479-1482. (c) De Mesmaeker, A.; Waldner, A.; Lebreton, J.; Hoffmann, P.; Fritsch, V.; Wolf, R.M.; Freier, S.M.; *Angew.Chem.Int.Ed.Engl.*, **1994**,*33*, 226-229. (d) Jones, R.J.; Lin, K.-Y.; Milligan, J.F.; Wadwani, S.; Matteucci, M.D. *J.Org.Chem.*,**1993**,*58*, 2983-2991. (e) Jones, R.J.; Swaminathan, S.; Milligan, J.F.; Wadwani, S.; Froehler,B.C.; Matteucci, M.D.; *J.Am.Chem.Soc.*, **1993**,*115*, 9816-9817. (f) Teng, K.; Cook, P.D.;*J.Org.Chem..*, **1994**,*59*, 278-280. (g) Veal, J.M.; Gao, X.; Brown, F.K.; *J.Am.Chem.Soc.*, **1993**, *115*, 7139-7145. (h) Chen, S.-M.; Mohan, V.; Kiely, J.S; Griffith, M.C.; Griffey, R.H.; *Tetrahedron Lett.* **1994**,*35*, 5105-5108. (i) Sanghvi, Y.S.; Cook, P.D. in: *Carbohydrate Modifications in Antisense Reserch*, ACS Symposium Series 580, ACS, Washington D.C., **1994**; pp 1-22.
8. Cummins,L.L.; personal communication.
9. de Leeuw, F.A.A.M.; van Beuzekom, A.A.; Altona,C.; *J. Comput. Chem.*,**1983**,*4*, 438-448.
10. Marion, D.; Ikura, M.; Tshudin,R.; Bax, A.; *J. Magn. Reson.*, **1989**,*85*, 393-399.
11. Davis, D.G.; Bax, A.; *J.Am.Chem.Soc.*, **1985**,*107*, 2820-2821.
12. Banks, K.M.,Hare, D.R.; Reid, B.R.; *Biochemistry.* **1989**, *28*, 6996-7010.
13. The partial atomic charges were assigned by a "donor-acceptor" scheme, using a fitting procedure to generate AMBER-like charges. Thacher, T.; BIOSYM Technologies, San Diego, CA 92121. *(personal communication)*
14. Walker, S.; Gange, D.; Gupta,V.; Kahne,D.; *J.Am.Chem.Soc.*, **1994**,*116*, 3197-3206.
15. Weiner, S.J.; Kollman, P.A.; Nguyen, D.T.; Case, D.A.; *J.Comput.Chem.*,**1986**,*7*, 230-252; as incorporated in the InsightII/ DISCOVER software from BIOSYM Technologies, San Diego, CA 92121.
16. Mohan, V.; Smith, P.E.; Pettitt, B.M.; *J.Am.Chem.Soc.*, **1993**,*115*, 9297-9298.
17. Mohan, V.; Smith, P.E.; Pettitt, B.M.; *J.Phys.Chem.*,**1993**,*97*, 12984-12990.

18. Swaminathan, S.; Ravishanker, G.; Beveridge, D.L.; *J.Am.Chem.Soc.*, **1991**,*113*, 5027-5040.
19. Van de Ven, F.J.M., Hilbers, C.W.;*Eur.J.Biochem*, **1988**, *178*, 1-38.
20. Fritsch, V.; Wolf, R.M.; *J.Biomol.Struct.Dyn.*, **1994**,*11*, 1161-1174.
21. Gorenstein, D.G.; Schroeder, S.A.; Fu, J.M.; Metz, J.T.; Roongta, V.; Jones, C.R.; *Biochemistry* , **1988**,*27*, 7223-7237.

(*Received in USA* 10 *March* 1995; *accepted* 25 *April* 1995)